Asian Journal of Chemistry; Vol. 37, No. 9 (2025), 2291-2297
ASIAN JOURNAL OF CHEMISTRY
https://doi.org/10.14233/ajchem.2025.34301

Carboxamide-Based Probe for Highly Selective Detection of Copper Ions: Synthesis, Spectroscopic Analysis, Theoretical Investigations and Catalytic Activity

SANKET KUMAR CHAKRAVARTI[1], VIBHA SHARMA[2], ABHAY NANDA SRIVASTVA[3], SOM SHANKAR DUBEY[1] and NETRA PAL SINGH[1,4,*]

[1]Department of Chemistry, D.D.U. Gorakhpur University, Gorakhpur-273009, India
[2]Department of Chemistry, N.A.S. (P.G.) College, Meerut-250003, India
[3]University Department of Chemistry, B.R.A. Bihar University, Muzaffarpur-842001, India
[4]Department of Chemistry, Dr. H.S. Gour Vishwavidyalaya, (A Central University), Sagar-470003, India

*Corresponding author: E-mail: npsmcm.in@gmail.com

Received: 21 June 2025 *Accepted*: 21 August 2025 *Published online*: 30 August 2025 AJC-22111

A carboxamide based fluorescent probe N^2,N^6-*bis*(5-(*p*-tolyl)thiazol-2-yl)pyridine-2,6-dicarboxamide was synthesized by the condensation reaction between pyridine-2,6-dicarboxylic and amino derivative of thiazole and characterized by FT-IR spectroscopy, ^{1}H NMR, ^{13}C NMR, UV-vis spectroscopy and LC-MS spectral studies. Absorption and fluorescence titrations were used to study the fluorescent. The probe exhibits high selectivity and sensitivity towards Cu^{2+} ions over a spectrum of metal ions (Cu^{2+}, Co^{2+}, Ni^{2+}, Hg^{2+}, Cr^{3+}, Al^{3+}, Fe^{2+}, Sn^{2+} and Pb^{2+}). Using Job's plot measurements, the binding stoichiometry mode of the probe with the Cu^{2+} ion was estimated to be 2:1. The Benesi-Hildebrand equation yielded a stability constant value of 8.252×10^7 M^{-2} for the fluorescent probe. It was found that the fluorescent probe's limit of detection (LOD) for the Cu^{2+} ion was 0.0242 µM. DFT analyses have also been performed to support the sensing technique. The Cu(II) complex's catalytic activity was assessed using the one-pot azide–alkyne cycloaddition click reaction in water without the use of any supplementary agents.

Keywords: Sensing, Catalytic activity, Chemosensor, Binding constant, Carboxamide ligand.

INTRODUCTION

Although many fluorescent and colorimetric chemosensors have been developed for the identification of heavy metal ions, researchers are still working to develop inexpensive and eco-friendly molecules [1-3]. These probes, which have different reactions to different metal ions, provide significant advantages for both *in vitro* and *in vivo* research due to their high selectivity and sensitivity, biological compatibility, ease of utilization and quick detection [4,5]. Copper (Cu^{2+}) is the third most prevalent transition metal ion in the human body, following ferrous (Fe^{2+}) and zinc (Zn^{2+}) ions, respectively [6]. It is essential for a number of biological functions, including acting as a cofactor for electron transfers in many proteins and a catalyst for redox reactions in biological pathways. The maximum acceptable concentration of Cu^{2+} ions in drinking water is 20 µM. However, excessive absorption of copper ions in humans can lead to serious neurological disorders, including Alzheimer's, Parkinson's, Huntington's and prion diseases [7]. Further, long exposure to copper ions may result in liver or kidney damage, along with digestive problems [8,9]. Due to the harmful effects on human health, fluorescence sensors for Cu^{2+} have attracted significant attention, resulting in the development of numerous devices for detecting copper pollutants in environmental settings, aquatic systems and cellular matrices [10-13]. Copper(II) ions is recognized as a fluorescence quencher due to its paramagnetic properties, leading most fluorescent chemosensors to detect Cu^{2+} by fluorescence quenching mechanisms [14-19].

Carboxamide ($R'CONR_2$), which are synthesized from carboxylic acid ($R'COOH$), represent an important functional group. Pyridine-2,6-dicarboxylic acid (PDC) is also known as dipicolinic acid (DPA), which acts as vital role in the heat resistance of bacterial endospores. Ligands based on pyridine-2,6-dicarb-

oxamide have been extensively used in different field of applications because such type of ligand have some unique features [20,21]. Through five membered chelated rings between the nitrogen of the pyridine and the nitrogen of amide groups, they have the ability to form a N^3 pincer cavity [22]. They form stable complexes in their higher oxidation state and also have possibilities to introduce assorted appended functional group on the amide atom to generate large number of interesting ligands [23]. From last decade, this field is much interesting for scientist because these types of ligand used in coordination chemistry as stabilization of reactive species, catalyst and sensing as well as in recognition.

2-Amino-4-(*p*-tolyl)thiazole is a compound that contains both a thiazole ring and a tolyl group. The amino group's existence suggests that it could be involved in various biological activities or serve as a building block in synthetic chemistry. However, fluorimetric and colorimetric dual-detection tests are now considered as promising candidates for the detection of heavy metal ions, including cobalt ions, because they cannot only offer a highly sensitive fluorescence evaluation of metal ions but also help in simple and affordable "naked eye" metal ion detection [24]. In addition to being essential for numerous biological functions, these ions have been shown to be deadly when present in excess of their acceptable limits [25].

EXPERIMENTAL

All analytical-grade reagents were acquired from Sigma-Aldrich, USA. All solvents used were also laboratory grade and were used without further purification. The Perkin-Elmer UV spectrometer was used to obtain the UV-visible spectra. Perkin-Elmer USA Spectrum, FTIR spectra were recorded. A JEOL, Japan 400 MHz spectrometer was used to acquire ^{1}H and ^{13}C NMR spectra. Using the SCIEX Triple TOF 5600 mass spectrometer, liquid chromatography-mass spectral analysis was performed. A quartz route length of 1 cm was used to record fluorescent spectra on a spectrofluorometer. The fluorescent sensor's stock solution was made with a 1 mM concentration of THF. At a concentration of 60 µM, the ligand exhibits saturation intensity. The chloride, acetate and nitrate salts of metal ions were combined with methanol to create a stock solution with a concentration of 2.5 mM. The Shimadzu RF 5301 PC spectrofluorophotometer features a quartz tube with a slit width of (5 nm) and a route length of (1 cm), was used to measure fluorescence. A Perkin-Elmer FT-IR spectrometer was used to collect the probe's infrared spectra using KBr in the 4000-400 cm^{-1} range. Using a Bruker Avance NEO 500 MHz spectrometer, the NMR spectra were recorded at ambient temperature.

Synthesis of probe: Probe was synthesized by reacting 2-amino-4-(*p*-tolyl)thiazole with pyridine-2,6-dicarboxylic acid. In brief, 20 mL of pyridine was mixed with 1.0 g of pyridine-2,6-dicarboxylic acid (0.0059 mol) and 2.27 g of 2-amino-4-(*p*-tolyl)thiazole (0.0118 mol) and refluxed for 30 min at 120 ºC. After adding $P(OPh)_3$ (3.844 g, 0.0125 mol) dropwise, the reaction mixture was agitated for 12 h at 80 ºC. The combination was allowed to normal to ambient temperature before being poured into ice-cold water, which resulted in the precipitation of a brown substance (**Scheme-I**). The product underwent filtering, multiple ethanol and water washes, vacuum drying and recrystallization in methanol. Yield: 90%, m.p.: 190 ºC; Elemental analysis of $C_{27}H_{21}N_5O_2S_2$: calcd. (found) %: C, 63.39 (63.41); H, 4.14 (4.25); N, 13.69 (13.71); O, 6.25 (6.32); S, 12.53 (12.61); ^{1}H NMR (500 MHz, DMSO, δ ppm): 8.85 (s, 2H, N-H), 8.23 (d, 2H), 7.57 (d, 4H), 7.40 (d, 4H) and 7.51 (t, 1H), 7.12 (s, 2H), (arom. protons, 13H, 7.0-8.3). ^{13}C NMR (DMSO, δ ppm): 150-120, (21C, arom. carbon), 168.41 (C=O), 157.32 (C=N), FT-IR (KBr, ν_{max}, cm^{-1}): 3580 (NH), 3200-2800 (C–H), 1496 (C=N) and 1645, 1624 (C=O). UV-vis (λ_{max}, nm); 257 and 328. LC-MS (*m/z*); Calcd. (found) for $C_{27}H_{21}N_5O_2S_2$: 511.11 (511.43).

Titration and sample preparation: The metal ions *viz.* Cu^{2+}, Co^{2+}, Ni^{2+}, Hg^{2+}, Cr^{3+}, Al^{3+}, Fe^{2+}, Sn^{2+} and Pb^{2+} solutions were prepared and conducted the titration studies at 1.0×10^{-3} M in CH_3COOH and their stock solutions (2.5 mM) were dissolved to 1.0×10^{-5} M. At room temperature, all the spectrum measurements were performed.

Optical studies: UV-vis and fluorescence spectroscopy were used to examine the synthesized probe's sensing behaviour toward different metal ions in methanol. The fluorescence spectra of the probe were recorded at an excitation wavelength of 341 nm with a slit width of 5 nm

DFT studies: Density functional theory (DFT) calculations were carried out using the ORCA 3.0.1 computational package [26]. In order to improve the geometry, the B3LYP functional was combined with Aldrich's def2–TZVP basis set

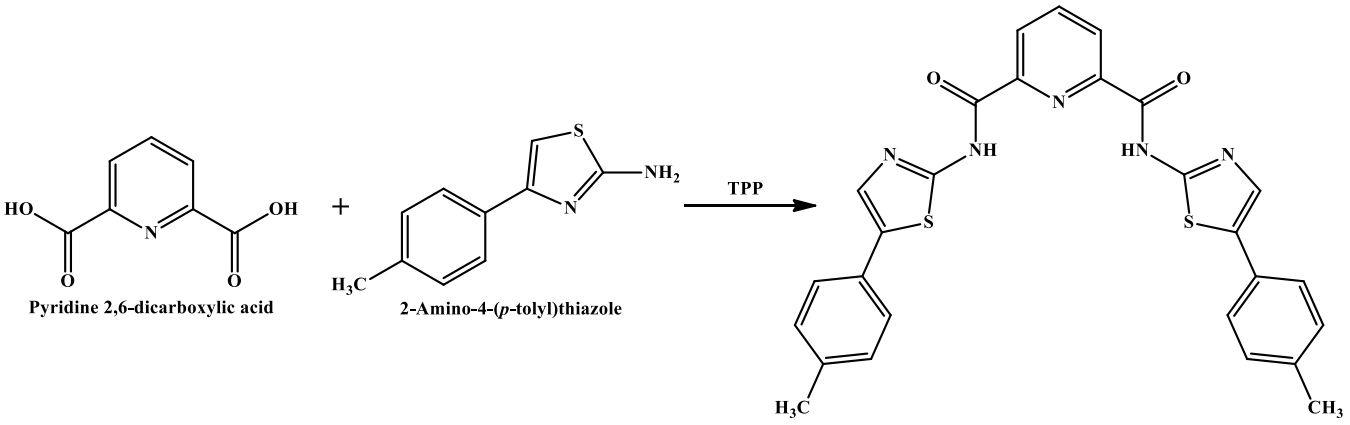

Scheme-I: Chemical structure of probe N^2,N^6-*bis*(5-(p-tolyl)thiazol-2-yl)pyridine-2,6-dicarboxamide

for copper atoms and def2–SVP basis set for C, H, O, N and S atoms. The def2–TZVP basis set for each atom was used to further recalculate the optimal structures in order to find the HOMO and LUMO energy. After the computations were completed, the energy-minimized geometry was built, optimized, and visualized using the Avogadro program [27].

Experimental procedure of CuAAC reaction: A standard approach involved dissolving an alkyne-functionalized molecule (1.0 mmol) and an amide-functionalized compound (1.0 mmol) in a 1:1 combination of water (5 mL) and *t*-butanol. To obtain Cu(I) *in situ*, sodium ascorbate (0.1 mmol, 19.8 mg) and copper(II) sulfate pentahydrate (0.05 mmol, 12.5 mg) were added to this solution. In a nitrogen environment, the reaction mixture was agitated for 12 to 24 h at room temperature. TLC was used to determine when the reaction was finished. Following completion, 10 mL of water was added to the reaction mixture and 3 × 10 mL of ethyl acetate was used for extraction. Anhydrous sodium sulfate was used to dry the mixed organic layers, after which they were filtered and concentrated under lower pressure. By using column chromatography (silica gel, hexane/ethyl acetate) to purify the crude product, the intended thiazole product was obtained in a good yield.

RESULTS AND DISCUSSION

The carboxamide-based sensor probe was synthesized in one step. The synthesized probe showed a brown colour and was soluble in a variety of organic solvents, such as DMSO, ethanol, methanol, chloroform and dichloromethane (DCM). Fluorescence spectroscopy and UV-vis were used to investigate the probe's sensing behaviour toward different metal ions in methanol.

FT-IR studies: FT-IR spectrum of probe (Fig. 1) shows the characteristic stretch peak at 3580 (NH) and 1645 (C=O), The peak value of stretching vibration found lower at 1496 (C=N), 3200-2800 (C–H) and 1323 (C=C).

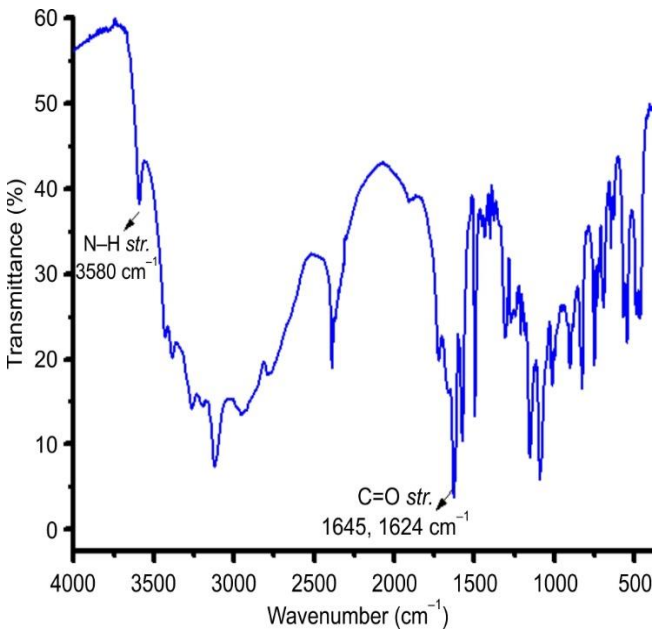

Fig. 1. IR spectrum of probe showing characteristic vibrational absorption peaks

UV-vis absorption studies: The π–π* and n–π* transitions associated with the tolyl chromophore is combined with the NH_2 group were identified as the source of two absorption bands', which were centered at 257 nm and 328 nm as shown in Fig. 2 [28].

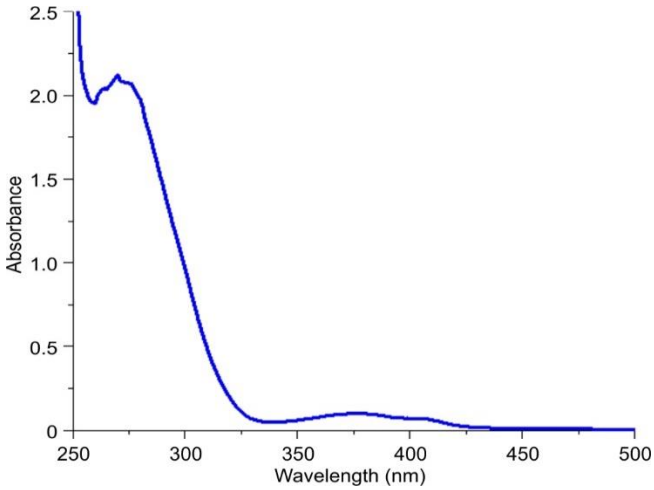

Fig. 2. UV-visible spectra of probe showing absorption characteristics across wavelengths

Fluorescence emission studies: The probe's selective fluorescence sensitivity toward several metal ions (Cu^{2+}, Co^{2+}, Ni^{2+}, Hg^{2+}, Cr^{3+}, Al^{3+}, Fe^{2+}, Sn^{2+} and Pb^{2+}), was examined following excitation at a wavelength of 328 nm. When the same amount of various metal ions was added to the probe's solution the wavelength significantly increased to the emission maximum observed at 520 nm, whereas the ligand's fluorescence intensity gradually decreased (Fig. 3). The fluorescence intensity of the probe was much enhanced by the chelation of Cu^{2+} ion with the NH_2 group, the nitrogen of the free NH_2 group and the corresponding imine bond C=N. Furthermore, through the chelation enhanced fluorescence (CHEF) effect, the binding of Cu^{2+} to the probe prevents the C=N isomerization and photoinduced electron transfer (PET) processes [29]. The fluorescence intensity expanded significantly up to 8 μM and remained constant, as a consequence of the fluorometric titration tests with Cu^{2+} being detected in a limited range of intensities 0-13 μM.

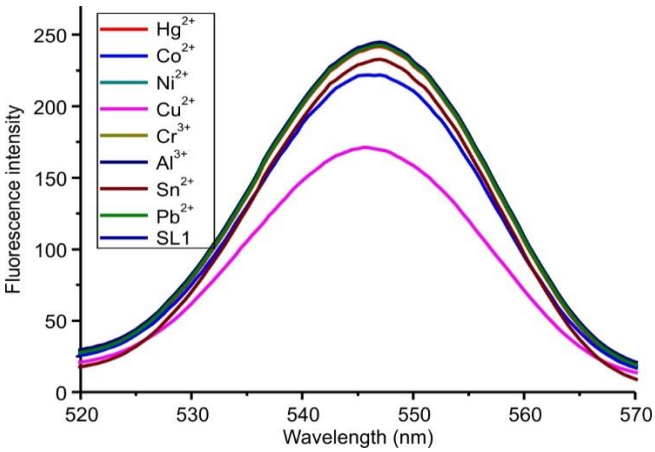

Fig. 3. Fluorescence emission spectra of probe with various metal ions

Effect of probe concentration and time-based response: The effect of probe's concentration on fluorescence intensity upon binding with the Cu^{2+} ion was observed while the probe's concentration increased from 1 to 12 µM. According to the results, the fluorescence intensity decreased as the probe's concentration increased and then stabilized at higher concentration (Fig. 4). In addition, the fluorescence intensity of probe and 1-Cu^{2+} was recorded with time. Although there were no apparent shifts for the probe, the fluorescence intensity of 1-Cu^{2+} enhanced rapidly, peaked in a matter of minutes and subsequently stabilized. This demonstrates clearly showed that the probe's response time for Cu^{2+} detection was fast.

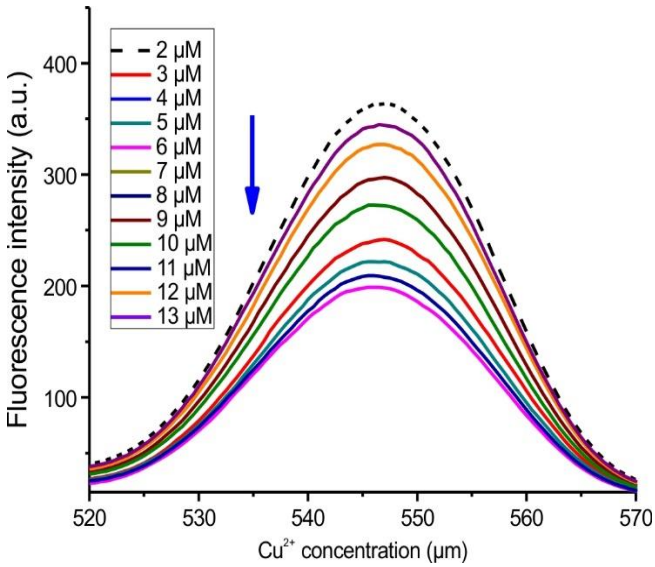

Fig. 4. Fluorescence emission spectrum of probe displaying intensity variations with increasing concentrations of Cu^{2+}

Studies of competitive binding using various metal ions: In a range of various metal ions (Cu^{2+}, Co^{2+}, Ni^{2+}, Hg^{2+}, Cr^{3+}, Al^{3+}, Fe^{2+}, Sn^{2+} and Pb^{2+}), competitive binding experiments were carried out in order for evaluating the functionality of the probe as a Cu^{2+} selective fluorescence sensor. The data clearly show that, with the exception of Cu^{2+} and Co^{2+}, there was minimal interference from other metal ions in Cu^{2+} detection. The slight decrease in Cu^{2+} and Co^{2+} fluorescence intensity is caused by electron or energy transfer [30]. According to the experimental findings, probe can be employed as a selective fluorescence sensor for Cu^{2+} detection even in the existence of various competitive metal ions.

Stoichiometry and probable binding mode: Job's plot method was used to explain the probe-Cu^{2+} complex's stoichiometry [31]. While the mole percentage fluctuated from 0.1 to 0.9 µM, the overall strength of probe-Cu^{2+} remained constant at 10 µM. Using the absorbance approach, the stoichiometry ratio was determined to be 2:1 for the Cu^{2+} complex, with emission maxima at a 0.3 molar ratio [32]. Using a nonlinear least square fit of the data, the association constant (K_a) was determined to be 8.252×10^7 M^2. Using the formula 3σ/k, where σ was the standard deviation of blank readings and k was the slope of the linear calibration curve, the range of detection for the probe was determined to be 0.0242 µM [33].

Confirmation of the sensing mechanism using spectroscopic studies: At room temperature, ^{1}H NMR analysis was performed in DMSO-d_6 solvent to confirm the binding and interaction characteristics of the probe. The addition of Cu^{2+} ions caused a downfield shift in the amine proton signal of the probe from 8.85 ppm to 8.95 ppm. Likewise, in the presence of the Cu^{2+} ion, the aromatic proton signal was observed in the 8.3-7.0 ppm range was likewise moved to an upfield region at 7.67-6.82 ppm. These modifications to the proton's chemical shifts in the presence of Cu^{2+} ions indicated that the probe's -NH and N atom of pyridine are the mechanism by which the probe and Cu^{2+} interact. LC-MS spectra of probe show peaks at 511.43. [Expected value, *m/z*: 511.11] (Fig. 5).

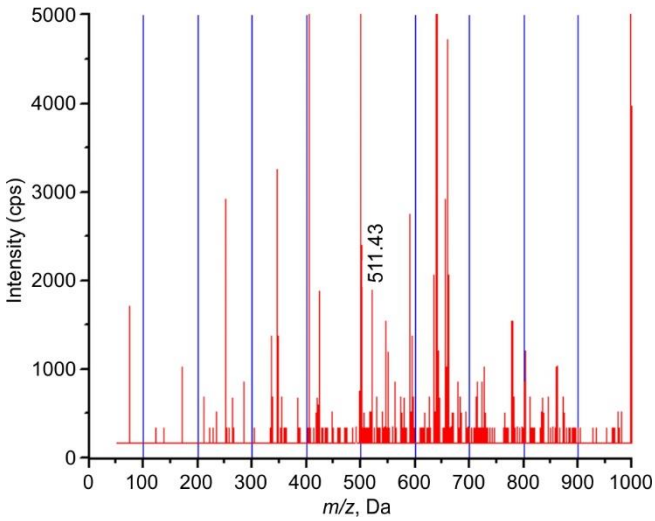

Fig. 5. LC-MS spectra of probe

Confirmation of sensing mechanism by DFT studies: The highest occupied molecular orbital (HOMO) and lowest unoccupied molecular orbital (LUMO) energies of Probe were determined, along with its kinetic and thermodynamic stability, using DFT studies. The optimized structure of probe obtained by DFT is shown in Fig. 6 and the associated parameters, specifically bond length and bond angle values, are listed in Table-1. The DFT results verified that the HOMO electron density is uniformly distributed over the fluff moiety along with the Cu^{2+} ion, while the LUMO electron density is primarily concentrated on the Cu^{2+} ion (Fig. 6). The energy gap between probe HOMO–LUMO has been calculated and determined to be 0.466 eV. The central metal ion coordinates with the two ligand moieties *via* carboxylic and NH_2 nitrogen atoms

TABLE-1
DETERMINED VALUES FOR THE PROBE'S REACTIVITY AND THERMODYNAMIC CHARACTERISTICS

Parameters	Probe
LUMO energy (eV)	0.771
HOMO energy (eV)	0.305
LUMO–HOMO energy (eV)	0.466
χ (eV)	0.466
µ (eV)	4.192
η (eV)	1.848
ω (eV)	1.515

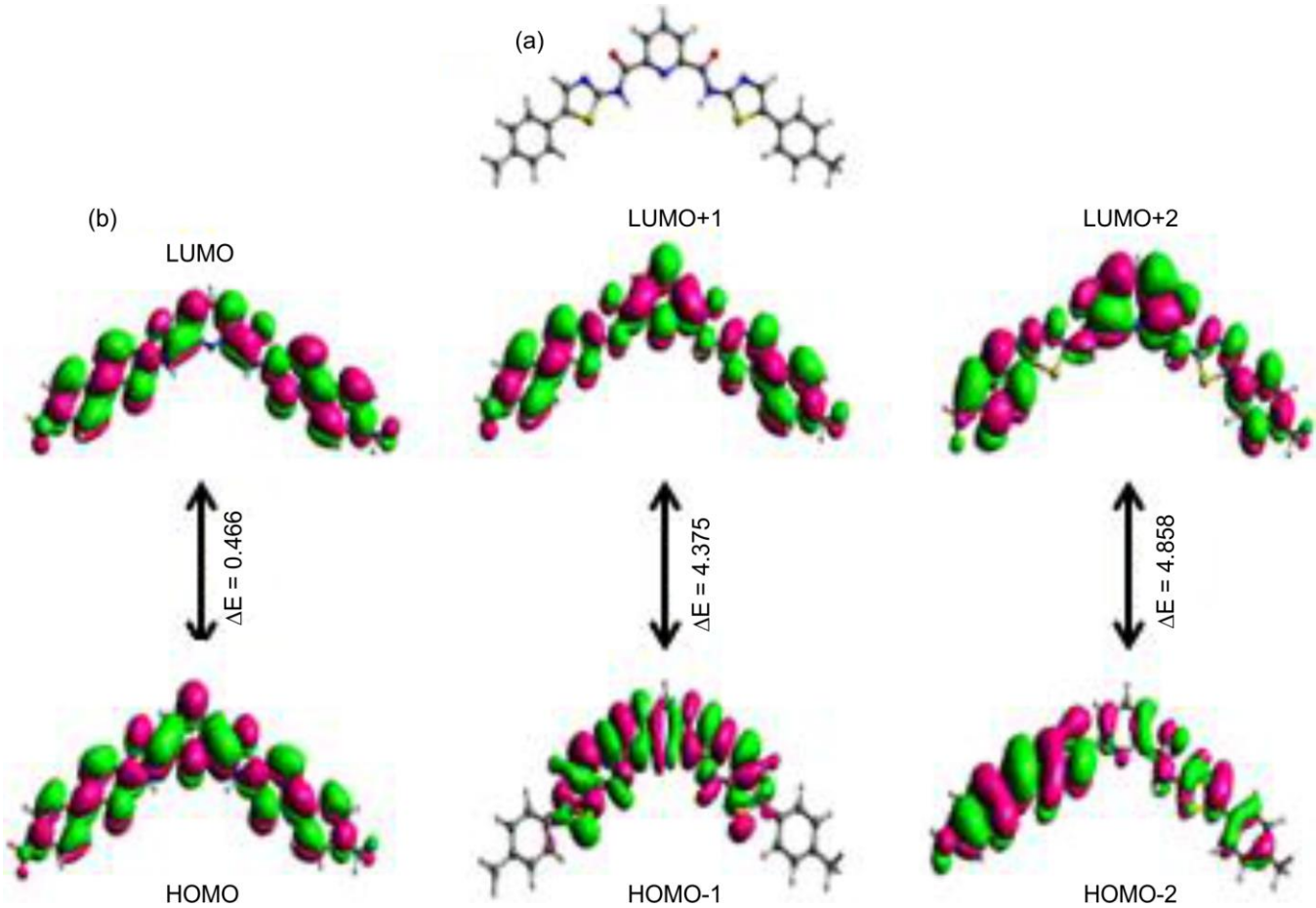

Fig. 6. (a) DFT-optimized geometry of probe. (b) Frontier molecular orbitals of probe, showing the energy difference between the (HOMO) and (LUMO)

as well as an oxygen atom, resulting in an octahedral shape, according to the probe's 2:1 binding stoichiometry with Cu^{2+}. According to the frontier orbital analysis, the HOMO orbital is primarily centered at the 2-amino-4-(*p*-tolyl)thiazole moiety, whilst the LUMO was found over the ligand's entire structure. After complexation, the 1–Cu^{2+} complex showed that the HOMO electrons were mostly adorned throughout the whole molecule, whereas the LUMO orbital was found to be localized around the metal center. As a result, the 1-Cu^{2+} complex displayed significant fluorescence activity and no electron transport.

Using DFT studies, the probe's IR spectra revealed the absorption peaks at 1496, 1624, 3089 and 3580 cm^{-1}, which were ascribed to the H–C=N, C=O and NH_2 groups. The probe's free –OH stretching vibration is the cause of the absence of the –OH band in the FT-IR spectrum [34]. The experimental spectrum acquired with the same shift show a good correlation with the theoretical values. From the geometry-optimized structures, the bond length and bond angles of the probe and 1-Cu^{2+} were determined. The bond length for –C=N in the probe instance was determined to be 1.284 Å, which stretched out to 1.320 Å upon coordination with Cu^{2+}. In contrast, the bond lengths for –C–N and –C–O decreased from 1.515 Å and 1.5143 Å to 1.505 Å and 1.471 Å, respectively. Likewise, C–N=C, C=C–N and C=C–O have bond angles of 122.16º, 119.11º and 126.86º, respectively, which shifted to 122.31º, 114.46º and 125.31º when they interact with Cu^{2+}. The binding of the ligand *via* pincer cavity nitrogen is thus further confirmed by the observed' changes in the bond lengths and bond angles of the probe upon complexation with Cu^{2+}.

Catalytic activity: By promoting the regioselective synthesis of N^2,N^6-*bis*(5-(*p*-tolyl)thiazol-2-yl)pyridine-2,6-dicarboxamide by the CuAAC reaction, the catalytic activity of the copper(I) species is crucial. Copper(II) sulfate pentahydrate and sodium ascorbate, which under mild circumstances converts Cu(II) to the catalytically active Cu(I) species, were used in this study to construct the catalytic system *in situ*.

By optimizing the catalyst loading to 5 mol% $CuSO_4$ and 10 mol% sodium ascorbate, the reactants were efficiently converted without the requirement for high temperatures or an inert atmosphere. Under typical reaction conditions, the catalytic system's excellent efficiency and recyclability were demonstrated by its high turnover numbers (TON) and turnover frequencies (TOF). According to kinetic studies, the cycloaddition reaction started quickly after the catalyst was added and was finished in 6-12 h at room temperature. It was found that the reaction was extremely tolerant of a large range of functional groups and chemoselective. The system's resilience and broad application were demonstrated by the catalytic activity's uniformity throughout a range of alkyne and azide substrates. The stability of the Cu(I) species produced *in situ*

TABLE-2
COMPARISON OF DIFFERENT CATALYTIC SYSTEMS FOR CuAAC REACTION [35]

Catalyst system	Reaction conditions	Yield (%)	Advantages	Drawbacks
$CuSO_4$/Sodium ascorbate	Room temperature, *t*-BuOH/H_2O	85-95	Mild conditions, clean reaction, easy to handle	Requires *in situ* generation of Cu(I)
CuI/CuBr	Room temperature, inert atmosphere	75-90	Pre-formed Cu(I), faster reaction	Air-sensitive, potential side reactions
Cu(0) (powder or turnings)	60-80 ºC, extended time	60-80	Inexpensive, readily available	Requires heat, heterogeneous mixture, slower rate
$CuSO_4$/Asc + TBTA or THPTA	Room temperature, aqueous/organic mixed media	90-98	High efficiency, water-soluble, biocompatible	Ligands may be costly or require separate synthesis

was demonstrated by the lack of a discernible decrease in catalytic performance upon reuse in subsequent cycles. These findings support the strong catalytic efficiency of the $CuSO_4$/sodium ascorbate system in promoting effective and regioselective thiazole synthesis *via* the CuAAC reaction (Table-2).

Correlation of probe with previous studies: The probe exhibited significantly better systematic performance than the previously reported ligands, according to a comparison with previously published Cu^{2+} sensors. The probe is more efficient to the selective detection of Cu^{2+} in various biological and environmental samples.

Conclusion

A new fluorescent probe based on carboxamide has been successfully synthesized and characterized with spectroscopic techniques like UV-vis spectroscopy and fluorescence titration measurements, the fluorescent probe demonstrated exceptional sensitivity to the selective detection of Cu^{2+} ions in the range of various metal ions. The limited C=N isomerization of the $–NH_2$ group was identified as the "turn-on" fluorescence mechanism in the presence of Cu^{2+}. This behaviour is attributed to fluorescence enhancement resulting from conformational restriction induced by coordination with the metal center, thereby strengthening the chelation effect. Job's plot was employed to determine the stoichiometry of complexation, revealing a 2:1 binding ratio between the probe and Cu^{2+}. An association constant of 8.252×10^7 M^{-2} was calculated for the probe–metal complex. According to WHO standards, the acceptable limit for Cu^{2+} (2 µM) is significantly higher than the detection limit of the probe, which was determined to be 0.0242 µM. For practical purposes, the probe can be used to identify lower Cu^{2+} amounts in water samples due to its lower detection limit. In mild conditions, the Cu(II)-complex catalyzed the azide–alkyne cycloaddition (AAC) reaction in water, producing high yields in a brief reaction time under aerobic conditions. As a result, the detection strategy presented here provides a practical method for the Cu^{2+} selective detection in different applications.

ACKNOWLEDGEMENTS

For providing the facilities of NMR and LC-MS, the authors are delightful to USIF, Aligarh Muslim University, Aligarh, India. The authors also acknowledge the granting FT-IR, UV-vis and fluorescence spectroscopic facilities by Department of Chemistry, DDU Gorakhpur University, Gorakhpur and Department of Chemistry at Aligarh Muslim University, Aligarh, India. The financial support provided by the R&D Higher Education Department under project grant no. 47/2021/606/ सत्तर-4-2021-4(56)/2020 is also gratefully acknowledged.

CONFLICT OF INTEREST

The authors declare that there is no conflict of interests regarding the publication of this article.

REFERENCES

1. S. Upadhyay, A. Singh, R. Sinha, S. Omer and K. Negi, *J. Mol. Struct.*, **1193**, 89 (2019); https://doi.org/10.1016/j.molstruc.2019.05.007
2. S. Nsanzamahoro, W. Cheng, F.P. Mutuyimana, L. Li, W. Wang, C. Ren, T. Yi, H. Chen and X. Chen, *Talanta*, **210**, 120636 (2020); https://doi.org/10.1016/j.talanta.2019.120636
3. E. Senkuytu and E.T. Eçik, *Spectrochim. Acta A Mol. Biomol. Spectrosc.*, **173**, 863 (2017); https://doi.org/10.1016/j.saa.2016.10.052
4. G. Singh, Sushma, Priyanka, Suman, Diksha, J.D. Kaur, A. Saini, A. Devi and P. Satija, *Inorg. Chim. Acta*, **525**, 120465 (2021); https://doi.org/10.1016/j.ica.2021.120465
5. S. Yang, W. Fan, D. Wang, Z. Gong and M. Fan, *Anal. Methods*, **11**, 3829 (2019); https://doi.org/10.1039/C9AY00709A
6. X. Xie, X. Chen, B. Li and L. Zhang, *Dyes Pigments*, **98**, 422 (2013); https://doi.org/10.1016/j.dyepig.2013.03.022
7. V. Desai and S.G. Kaler, *Am. J. Clin. Nutr*., **88**, 855S (2008); https://doi.org/10.1093/ajcn/88.3.855S
8. K. Ghosh and D. Kar, *J. Incl. Phenom. Macrocycl. Chem*., **77**, 67 (2012); https://doi.org/10.1007/s10847-012-0217-6
9. Y. Zheng, K.M. Gattas-Asfura, V. Konka and R.M. Leblanc, *Chem. Commun*., 2350 (2002); https://doi.org/10.1039/B208012E
10. M. Saleem, M. Rafiq, M. Hanif, M.A. Shaheen and S.-Y. Seo, *J. Fluoresc*. **28**, 97 (2018); https://doi.org/10.1007/s10895-017-2178-z
11. S. Chowdhury, B. Rooj, A. Dutta and U. Mandal, *J. Fluoresc*., **28**, 999 (2018); https://doi.org/10.1007/s10895-018-2263-y
12. K.P. Carter, A.M. Young and A.E. Palmer, *Chem. Rev*., **114**, 4564 (2014); https://doi.org/10.1021/cr400546e
13. E.V. Antina, N.A. Bumagina, A.I. V'Yugin and A.V. Solomonov, *Dyes Pigments*, **136**, 368 (2017); https://doi.org/10.1016/j.dyepig.2016.08.070
14. A. Torrado, G.K. Walkup and B. Imperiali, *J. Am. Chem. Soc*., **120**, 609 (1998); https://doi.org/10.1021/ja973357k
15. G. Klein, D. Kaufmann, S. Schürch and J.-L. Reymond, *Chem. Commun*. 561 (2001); https://doi.org/10.1039/B100535I

16. M. Boiocchi, L. Fabbrizzi, M. Licchelli, D. Sacchi, M. V´azquez and C. Zampa, *Chem. Commun*., 1812 (2003); https://doi.org/10.1039/B305456J
17. Y. Zheng, J. Orbulescu, X. Ji, F.M. Andreopoulos, S.M. Pham and R.M. Leblanc, *J. Am. Chem. Soc*., **125**, 2680 (2003); https://doi.org/10.1021/ja0293610
18. B.C. Roy, B. Chandra, D. Hromas and S. Mallik, *Org. Lett*., **5**, 11 (2003); https://doi.org/10.1021/ol026891s
19. S.H. Kim, J.S. Kim, S.M. Park and S.-K. Chang, *Org. Lett*., **8**, 371 (2006); https://doi.org/10.1021/ol052282j
20. T.C Harrop and P.K. Mascharak, *Acc. Chem. Res*., **37**, 253 (2004); https://doi.org/10.1021/ar0301532
21. A. Rajput and R. Mukherjee, *Coord. Chem. Rev*., **257**, 350 (2013); https://doi.org/10.1016/j.ccr.2012.03.024
22. D.S. Marlin and P.K. Mascharak, *Chem. Soc. Rev*., **33**, 539 (2000); https://doi.org/10.1039/A905282H
23. P.J. Donoghue, J. Tehranchi, C.J. Cramer, R. Sarangi. E.I. Solomon and W.B. Tolman, *J. Am. Chem. Soc*., **133**, 17602 (2011); https://doi.org/10.1021/ja207882h
24. B. Dar, S. Sharif, M. A. Khurshid, S. Hussain, B. Riaz, M. Musaffa, H. Khalid, A.R. Cha and A. Mahboob, *RSC Adv*., **14**, 9819 (2024); https://doi.org/10.1039/D4RA00445K
25. W. Liu, J. Chen, L. Xu, J. Wu, H. Xu, H. Zhang and P. Wang, *Spectrochim. Acta A Mol. Biomol. Spectrosc.*, **85**, 38 (2012); https://doi.org/10.1016/j.saa.2011.08.071
26. F. Neese, *Wiley Interdiscip. Rev. Comput. Mol. Sci*., **2**, 73 (2012); https://doi.org/10.1002/wcms.81
27. M.D. Hanwell, D.E. Curtis, D.C. Lonie, T. Vandermeersch, E. Zurek and G.R. Hutchison, *J. Cheminform*., **4**, 2 (2012); https://doi.org/10.1186/1758-2946-4-17
28. K. Tayade, S.K. Sahoo, S. Chopra, N. Singh, B. Bondhopadhyay, A. Basu, N. Patil, S. Attarde and A. Kumar, *Inorg. Chim. Acta*, **421**, 538 (2014); https://doi.org/10.1016/j.ica.2014.05.014
29. S. Sinha, R. R. Koner, S. Kumar, J. Mathew, P.V. Monisha, I. Kazia and S. Ghosh, *RSC. Adv*., **3**, 345 (2013); https://doi.org/10.1039/C2RA21967K
30. G. Dong, K. Duan, Q. Zhang and Z. Liu, *Inorg. Chim. Acta*, **487**, 322 (2019); https://doi.org/10.1016/j.ica.2018.12.036
31. H. Wang, D. Wang, Q. Wang, X. Li and C.A. Schalley, *Org. Biomol. Chem*., **8**, 1017 (2010); https://doi.org/10.1039/B921342B
32. L.M. Liu and Z.Y. Yang, *Inorg. Chim. Acta*, **469**, 588 (2018); https://doi.org/10.1016/j.molstruc.2022.134329
33. S. Zehra, R.A Khan, A. Alsalme and S. Tabassum, *J. Fluorosc*., **29** 1029 (2019); https://doi.org/10.1039/C9RA06356K
34. M. Asadi and M.S. Khah, *J. Iran. Chem. Soc*., **7**, 875 (2010); https://doi.org/10.1007/BF03246082
35. M. Kiani, M. Bagherzadeh, S. Meghdadi, F. Fadaei-Tirani, M. Babaie and K. Schenk-Joß, *Inorg. Chim. Acta*, **506**, 119514 (2020); https://doi.org/10.1016/j.ica.2020.119514